

Charge storage in spinless solitons in $trans\text{-(CH)}_x$: *In situ* magnetic-resonance measurements during p -type electrochemical doping

J. Chen and A. J. Heeger

Department of Physics and Institute for Polymers and Organic Solids,
University of California, Santa Barbara, California 93106

(Received 26 August 1985)

In situ measurements of the electron-spin resonance of $[(\text{CH})^y+(\text{ClO}_4^-)_y]_x$ during electrochemical doping are reported. The results demonstrate that charge is stored in a spinless configuration for p -type doping at concentrations below about 6 mol%. These magnetic data, therefore, support the conclusions of earlier studies indicating that doping of $trans\text{-(CH)}_x$ occurs via the formation of spinless charged solitons. Comparison of the results obtained from p - and n -type doping confirms the charge-conjugation symmetry of polyacetylene.

I. INTRODUCTION

Experimental studies have demonstrated that in doped $trans\text{-(CH)}_x$ charge is stored in the mid-gap states of doping-induced solitons.¹ Specific evidence of the existence of the mid-gap state has been obtained from spectroscopic studies of samples doped with a variety of dopants,¹ both n and p type. Equally important are the magnetic studies which, for carefully doped samples, have demonstrated²⁻⁴ charge storage in a spinless configuration, consistent with the reversed spin-charge relationship⁵ of the topological solitons of $trans$ -polyacetylene.

The initial spin-resonance experiments⁶ implying spinless charge carriers were carried out on p -type samples and utilized AsF_5 vapor-phase doping. The interpretation of these early experiments⁶ was controversial⁷ because of the possibility of nonuniform doping with AsF_5 vapor, the use of thick films (thickness comparable to the microwave skin depth), and the complex chemistry of AsF_5 doping. To avoid these problems, subsequent work in our laboratory²⁻⁴ has utilized *in situ* ESR measurements of thin films (thickness of order 1 μm or less) carried out on n -type $[\text{Na}_y+(\text{CH})^y]_x$ during electrochemical doping. The results²⁻⁴ of these measurements demonstrated unambiguously the spinless character of the doping-induced charged states at dilute doping concentrations and, together with parallel measurements carried out during photoexcitation,^{8,9} established the reversed spin-charge relation for solitons in $trans\text{-(CH)}_x$.

In this paper, we describe results obtained by applying these same techniques to p -type doping; *in situ* ESR measurements on $[(\text{CH})^y+(\text{ClO}_4^-)_y]_x$ during electrochemical doping. Consistent with the expected charge-conjugation symmetry of $trans\text{-(CH)}_x$, the data once again demonstrate charge storage at dilute concentrations in the spinless mid-gap states of charged solitons.

II. EXPERIMENTAL TECHNIQUES

The techniques used for these measurements are similar to those developed earlier^{3,4} for *in situ* ESR experiments on $[\text{Na}_y+(\text{CH})^y]_x$ during electrochemical doping; only the solvent and electrolyte were changed. The $(\text{CH})_x$ sample, electrolyte (0.3 M NaClO_4^- in propylene carbonate) and

counterelectrode (Na metal) were assembled (in a controlled atmosphere dry box) inside a 3 mm ESR tube and then sealed under dynamic vacuum with the tip of the cell frozen in liquid nitrogen. The $(\text{CH})_x$ electrode was a thin film (about 2 μm thickness) polymerized on a conducting (indium/tin oxide coated) quartz substrate using techniques described earlier.¹⁰ In order to achieve cell stability and to avoid side reactions, all experiments were restricted to cell voltages less than or equal to 3.50 V (versus Na). At higher voltages, clear indications of cell instability were observed [e.g., discoloration of the $(\text{CH})_x$ and counterelectrodes, and increasing background currents]. The doping concentrations were therefore limited to the dilute to intermediate regimes. To estimate values for the concentrations (y), we used the electrochemical calibration for $[(\text{CH})^y+(\text{ClO}_4^-)_y]_x$ obtained earlier.¹¹ The voltage scale was then shifted to account for the difference in electrochemical potential of Li (used for the counterelectrode in the earlier studies¹¹) and Na used as the counterelectrode in the present experiments. As a result, there is some uncertainty in the y values, particularly at the higher doping levels. From analysis of the electrochemical and magnetic data, we conclude that in these experiments $y_{\text{max}} \approx 0.06 \pm 0.01$. At lower cell voltages (and more dilute concentrations), the uncertainty in y is considerably smaller. However, the controlled variable in these experiments is the electrochemical potential of the polymer (the cell open-circuit voltage) which can be set and reproduced with arbitrarily high accuracy.

The large dielectric constant of propylene carbonate ($\epsilon \approx 65$) introduces a major perturbation into the cavity leading to a large frequency shift, loss of Q , and excess noise. In order to avoid these problems and maintain sufficient sensitivity, quartz beads were filled into the bottom part of the cell so as to minimize the solvent volume in the cavity.

The spin-resonance data were taken by first setting the external voltage and monitoring the current while allowing the cell to approach equilibrium over a period of typically 12 h. After stepping the voltage by $\Delta V = 0.1$ V, the initial current for voltages beyond the injection threshold at ≈ 3 V was 4 μA falling to < 0.1 μA as the cell approached equilibrium. At equilibrium, the measured external voltage is the open circuit voltage which is, by definition, the electrochemical potential of the doped polymer referenced to that

of the Na counterelectrode. After allowing the cell to come to equilibrium, the ESR signal was recorded using signal averaging to obtain the necessary signal-to-noise ratio from the thin-film samples. The spin resonance was made with an IBM Instruments E-200D ESR spectrometer interfaced to an Apple IIe computer for signal averaging and data analysis. The ESR derivative signal was integrated twice to obtain the spin susceptibility (χ_s). A National Bureau of Standards ruby standard was attached to the outside of the ESR tube (near the sample) for calibration of the absolute value of the magnetic susceptibility. Symmetric ESR lines and accurate χ values were obtained since the sample thickness ($\approx 2 \mu\text{m}$) was carefully limited to be much less than the microwave skin depth even at the highest concentrations.

III. EXPERIMENTAL RESULTS

The spin contribution to the magnetic susceptibility and the ESR linewidth data shown in Figs. 1 and 2 were obtained from doping and undoping cycles (each cycle is denoted with a different symbol) with two independent samples. Figure 1 shows the measured magnetic (spin) susceptibility as a function of the electrochemical potential (μ) of the doped polymer, and Fig. 2 shows the linewidth as a function of μ . The *p*-type injection threshold for *trans*-(CH)_x was determined in earlier electrochemical experiments¹² to be about 3 V (versus Li). Since the cell used in the *in situ* ESR experiments uses a Na counterelectrode, the threshold is expected to be at about 2.7 V. This onset of doping shows up in Fig. 2 as the cell voltage at which ESR line narrowing begins.

The electrochemical cells were stable over a period of approximately six weeks, and both χ and ΔH_{pp} values were reproducible from cycle to cycle and from sample to sample. The data are quantitatively similar to the results for χ and ΔH vs μ obtained from electrochemical doping^{3,4} of [Na_y⁺(CH)^{y-}]_x for comparable dopant concentrations.

The initial susceptibility of *trans*-(CH)_x due to neutral solitons decreased slightly from 3.5×10^{-7} emu/mol to about 2.2×10^{-7} emu/mol for μ beyond 3 V. For voltages beyond 3.0 V (with respect to Na), the number of spins was independent of μ (and thus independent of y), with a value identical to that obtained in the analogous *in situ n*-type

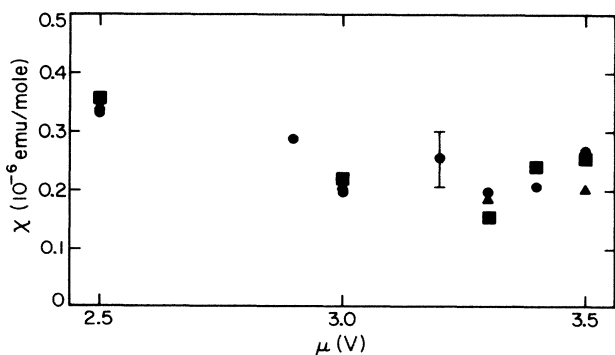


FIG. 1. Electron-spin contribution to the magnetic susceptibility for *p*-type [(CH)^{y+}(ClO₄⁻)_y]_x plotted as a function of the electrochemical potential, μ , of the polymer (referenced to Na). ■, sample 1, doping; ●, sample 2, cycle 1 (doping and undoping); ▲, sample 2, cycle 2 (doping and undoping).

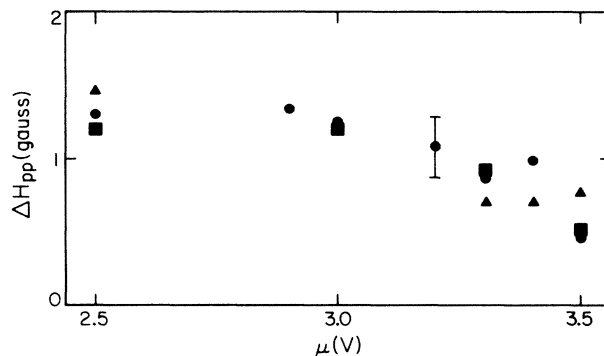


FIG. 2. Peak-to-peak ESR linewidth, ΔH_{pp} , for *p*-type [(CH)^{y+}(ClO₄⁻)_y]_x plotted as a function of the electrochemical potential, μ , of the polymer (referenced to Na); symbols as defined for Fig. 1.

doping experiments.²⁻⁴ Independent measurements have demonstrated that for the dilute to intermediate concentrations of Figs. 1 and 2 the susceptibility follows Curie's law.¹³ We suggested earlier^{4,14} that this concentration-independent Curie contribution may arise from formation of one kinetically metastable spin- $\frac{1}{2}$ polaron per two (CH)_x chains, since at any dopant level approximately half the chains will have an odd number of charges. The observation that the same value is observed independent of dopant and for both *n*- and *p*-type doping implies that the number of spins is a property of the (CH)_x chains, consistent with this interpretation. Moreover, the observed spin number (\sim one-to-two per 10⁴ carbon atoms) is consistent with the average molecular weight¹⁵ of (CH)_x prepared by the Shirakawa method.

IV. DISCUSSION

Transport studies¹³ of [(CH)^{y+}(ClO₄⁻)_y] have shown the increase in electrical conductivity characteristic of doped polyacetylene; for $y \approx 0.04$, electrochemically doped samples yield $\sigma \approx 20 \Omega^{-1}\text{cm}^{-1}$ at room temperature. This major increase in conductivity clearly indicates mobile charge carriers. The *in situ* spectroscopic studies¹¹ carried out during electrochemical doping with (ClO₄⁻) showed the characteristic growth of the mid-gap absorption and the associated decrease of oscillator strength in the interband transition, quantitatively consistent with charge storage in the mid-gap states of solitons. The susceptibility data of Fig. 1 demonstrate that in the dilute to intermediate doping regime charge is stored predominantly in a nonmagnetic configuration, for example, at a cell voltage of about 3.5 V, $N_s/N_{\text{CH}} < 2 \times 10^{-3}$. The results, therefore, demonstrate that for both *p*- and *n*-type charge injection, doping occurs via the formation of spinless charged solitons.

The data of Fig. 1 are qualitatively similar to those reported by Yang *et al.*¹³ In that study, the [(CH)^{y+}(ClO₄⁻)_y]_x samples were prepared electrochemically and subsequently removed from the electrochemical cell (Pt counterelectrode) for use in physical measurements. The results obtained *in situ* (Fig. 1) show that χ remains small throughout the experimental range studied with no indication of the small pretransitional increase in χ reported by Yang *et al.*¹³ Since the *in situ* technique using extremely thin films and a well-defined simple reaction at the coun-

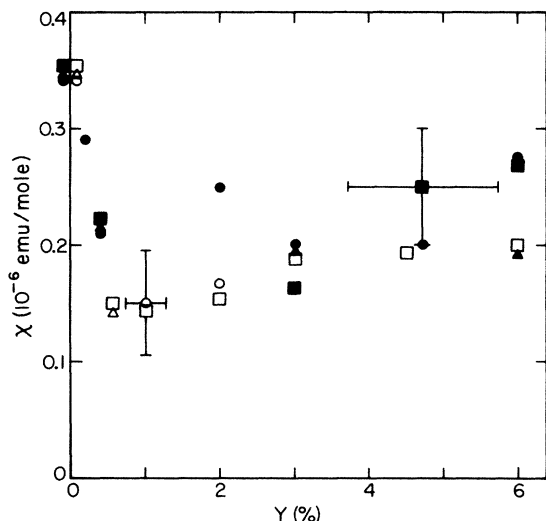


FIG. 3. Comparison of the magnetic (spin) susceptibility vs dopant concentration, y , for n - and p -type doping; $[(\text{Li}_y^+(\text{CH})^{y-})_x]$ and $[(\text{CH})^{y+}(\text{ClO}_4^-)_y]_x$, respectively. The data points denote different samples and different cycles. $[(\text{Li}_y^+(\text{CH})^{y-})_x]$: \square , doping; \circ , undoping; Δ , redoping. $[(\text{CH})^{y+}(\text{ClO}_4^-)_y]_x$: \blacksquare , sample 1, doping; \bullet , sample 2, cycle 1 (doping and undoping); \blacktriangle , sample 2, cycle 2 (doping and undoping).

terelectrode should provide the best control of dopant concentration and optimum dopant uniformity, the smaller and concentration-independent χ values shown in Fig. 1 are more nearly characteristic of the ideal situation. Thus, as in the case²⁻⁴ in $[\text{Na}_y^+(\text{CH})^{y-}]_x$, the Pauli contribution to the susceptibility remains small throughout the intermediate doping regime with no indication of a finite density of states in the gap. The magnetic data for p -type doping, therefore, further support the argument^{4,16} that the transport in this regime is due to mobile spinless solitons rather than due to hopping of electrons (or holes) through disorder-induced gap states.¹⁷

As discussed above, cell stability restricted the dopant concentration to less than about 6% so that we were unable

to reach the transition to a finite Pauli susceptibility. Yang *et al.*¹³ reported typical values for χ_p at concentrations above 6% with a rounded transition. The data of Fig. 1 suggest that the onset of χ_p may be abrupt for $[(\text{CH})^{y+}(\text{ClO}_4^-)_y]_x$ as was the case for Na doping.²⁻⁴ Experiments are underway directed toward design of a cell with working electrode, electrolyte, and well-defined counter-electrode all stable to higher (ClO_4^-) concentrations.

In Fig. 3, we plot χ vs y for p -type $[(\text{CH})^{y+}(\text{ClO}_4^-)_y]_x$. The concentration values were obtained by direct electrochemical calibration of V vs y as described in Sec. II. For comparison, we plot similar data obtained for $[(\text{Li}_y^+(\text{CH})^{y-})_x]$, where again the y values were obtained by direct electrochemical calibration.¹⁸ The data for Li doping were obtained using the *in situ* ESR technique (with 0.3 M LiClO_4 in THF and a lithium counterelectrode). We compare the p - and n -type data for (ClO_4^-) and Li^+ doping, respectively, in Fig. 3, since in both cases the electrochemical V vs Q curves are smooth with no indication of the well-defined plateaus¹⁹ observed with Na and K doping. The excellent agreement of the two sets of data confirms the charge-conjugation symmetry expected for polyacetylene.

V. CONCLUSION

In summary, the magnetic (spin) susceptibility and ESR linewidth were obtained as a function of the electrochemical potential through *in situ* measurements on $[(\text{CH})^{y+}(\text{ClO}_4^-)_y]_x$ during p -type doping. The results show that charge is stored in spinless solitons at concentrations below about 6%. Comparison of results obtained from p -type and n -type doping confirms the charge-conjugation symmetry of polyacetylene. The data imply that the Pauli contribution to the susceptibility remains small throughout the intermediate doping regime with no indication of a finite density of states in the gap.

ACKNOWLEDGMENT

These magnetic resonance studies were supported by the National Science Foundation, Grant No. DMR82-12800.

¹For brief reviews summarizing the spectroscopic and magnetic data, see the following: (a) S. Etamad, A. J. Heeger, and A. G. MacDiarmid, *Annu. Rev. Phys. Chem.* **33**, 443 (1982); (b) A. J. Heeger, *Phil. Trans. R. Soc. London, Ser. A* **314**, 17 (1985).

²T.-C. Chung, F. Moraes, J. D. Flood, and A. J. Heeger, *Phys. Rev. B* **29**, 2341 (1984).

³J. Chen, T.-C. Chung, F. Moraes, and A. J. Heeger, *Solid State Commun.* **53**, 757 (1985).

⁴F. Moraes, J. Chen, T.-C. Chung, and A. J. Heeger, *Synth. Met.* **11**, 271 (1985).

⁵W. P. Su, J. R. Schrieffer, and A. J. Heeger, *Phys. Rev. Lett.* **42**, 1698 (1979); *Phys. Rev. B* **22**, 2099 (1980).

⁶S. Ikehata, J. Kaufer, T. Woerner, A. Pron, M. A. Dray, A. Sivak, A. J. Heeger, and A. G. MacDiarmid, *Phys. Rev. Lett.* **45**, 1123 (1980).

⁷(a) Y. Tomkiewicz, T. D. Schultz, H. B. Broom, T. C. Clarke, and G. B. Street, *Phys. Rev. Lett.* **43**, 1532 (1979); (b) Y. Tomkiewicz, T. D. Schultz, H. B. Broom, A. R. Taranko, T. C. Clarke, and G. B. Street, *Phys. Rev. B* **24**, 4348 (1981).

⁸J. D. Flood and A. J. Heeger, *Phys. Rev. B* **28**, 2356 (1983).

⁹F. Moraes, Y. W. Park, and A. J. Heeger, in *Proceedings of the Workshop on Synthetic Metals III, Los Alamos, New Mexico, 1985* [*Synth. Met.* (to be published)].

¹⁰T.-C. Chung, Ph.D. thesis, University of Pennsylvania, 1982 (unpublished).

¹¹A. Feldblum, J. H. Kaufman, S. Etamad, A. J. Heeger, T.-C. Chung, and A. G. MacDiarmid, *Phys. Rev. B* **26**, 815 (1982).

¹²J. H. Kaufman, J. W. Kaufer, A. J. Heeger, R. Kaner, and A. G. MacDiarmid, *Phys. Rev. B* **26**, 2327 (1982).

¹³X. Q. Yang, D. B. Tanner, M. J. Rice, H. W. Gibson, A. Feldblum, and A. J. Epstein (unpublished).

¹⁴F. Moraes, D. Davidov, M. Kobayashi, T.-C. Chung, J. Chen, A. J. Heeger, and F. Wudl, *Synth. Met.* **10**, 169 (1985).

¹⁵J. C. W. Chien, M. Schen, and F. Karasz, *Makromol. Chem.* **5**, 217 (1984).

¹⁶D. Moses, A. Denenstein, J. Chen, P. McAndrew, T. Woerner, A. J. Heeger, A. G. MacDiarmid, and Y. W. Park, *Phys. Rev. B* **25**, 7652 (1982).

¹⁷A. J. Epstein, H. Rommelmann, R. Bigelow, H. W. Gibson, D. M. Hoffmann, and D. B. Tanner, *Phys. Rev. Lett.* **50**, 1866 (1983).

¹⁸R. Kaner and A. G. MacDiarmid, *J. Chem. Soc. Faraday Trans. 1*, **80**, 2109 (1984).

¹⁹(a) L. W. Shacklette, J. E. Toth, N. S. Murthy, and R. H. Baughman, *J. Electrochem. Soc.* **132**, 1529 (1985); (b) R. H. Baughman, L. W. Shacklette, N. S. Murthy, G. G. Miller, and R. L. Eisenbaumer, *Mol. Cryst. Liq. Cryst.* **120(B)**, 253 (1985).